

Supporting Information (SI)

Rational design of type-I photosensitizer molecules for mitochondrion-targeted photodynamic therapy

Jiaxin Liang^a, Xiaoyun Ran^a, Yanhong Liu^a, Xiaoqi Yu^b, Shanyong Chen^{a*} and Kun Li^{a*}

^aKey Laboratory of Green Chemistry and Technology, Ministry of Education, College of Chemistry, Sichuan University, Chengdu, 610064, China.

E-mail: chensy@scu.edu.cn (S.Chen), kli@scu.edu.cn (K. Li)

^bAsymmetric Synthesis and Chiral Technology Key Laboratory of Sichuan Province, Department of Chemistry, Xihua University, Chengdu, Sichuan 610064, China.

1. General information

1.1 Materials and Instruments.

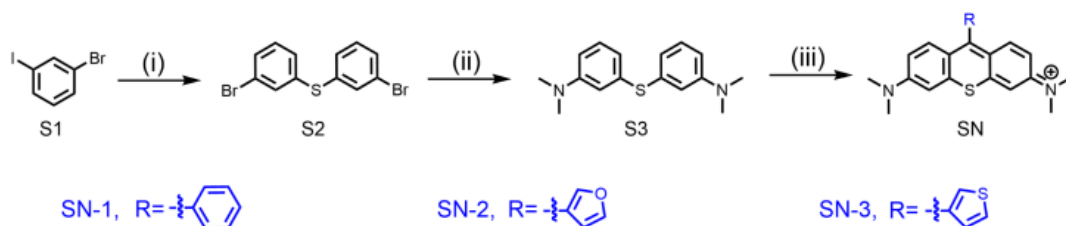
All chemicals and reagents were commercially available and used as received without further purification. The intermediate compounds were synthesized according to the previously reported procedures. 2',7'-Dichlorodihydrofluorescein diacetate (DCFH-DA), Dihydroethidium (DHE), 9,10-Anthracenediyl-bis(methylene)dimalonic Acid (ABDA) and Cell Counting Kit-8 (CCK-8) were purchased from Sigma-Aldrich and used as received. For cell culture, fetal bovine serum (FBS), penicillin–streptomycin solution, and Mito Tracker Green, Mitochondrial membrane potential assay kit, Annexin V-FITC Apoptosis Detection Kit with JC-1 and Calcein/PI Cell Viability/Cytotoxicity Assay Kit were purchased from Beyotime. ¹H and ¹³C NMR spectra were measured on a Bruker ARX 400 NMR spectrometer using CDCl₃ as solvents, and tetramethylsilane (TMS; δ = 0 ppm) was chosen as the internal reference. UV-vis absorption spectra were recorded on a Duetta (HORIBA) spectrometer. Fluorescence emission spectra were recorded on a Fluorolog-3 (HORIBA) spectrofluorometer. CCK-8 assay was monitored by the microplate reader (SPARK, Tecan, Switzerland). Irradiation was performed by using a LED light (560-565 nm). The simulation was carried out with the Gaussian 09 package. Confocal lasing scanning microscopic (CLSM) images of single-photo were obtained using LSM 780 (Zeiss) and analyzed using ZEN 3.4 software (Carl Zeiss).

1.2 Ethical statement

The animal experiments were carried out according to the protocol approved by the Ministry of Health in the People's Republic of PR China and were approved by Ethical Committees of West China School of Stomatology, Sichuan University (KS2022234).

1.3 Procedures and characterizations data of compounds.

SN derivatives were synthesized following a multi-step synthesis scheme S1. Intermediate products were collected at each step and characterized for identity and purity. Each step of the reaction scheme is described briefly below.



Scheme. S1. Synthetic route of SN derivatives. Conditions: (i) Na₂S·9H₂O, CuI, K₂CO₃, DMF, 130 °C 12 h; (ii) Dimethylamine, CuI, K₂CO₃, L-Proline, DMSO, 100 °C, 12 h; (iii) Aldehyde derivatives, p-Toluenesulfonic acid monohydrate, AcOH, 140 °C, 12 h, Chloranil, MeOH, 30 min.

Synthesis of compound S2: Compound S1 (20 g, 70.7 mmol), Sodium sulfide nonahydrate (11 g, 45.8 mmol), Copper(I) iodide (1.4 g, 7 mmol) and then Potassium carbonate (10.5 g, 76 mmol) was added in a Two-necked flasks. The flask was evacuated and backfilled with Ar for three times. N,N-Dimethylformamide (80 mL) was added via syringe through the septum. The reaction mixture was heated to 130 °C until S1 had been completely consumed by TLC analysis. At this point the reaction mixture was allowed to cool to room temperature, It was then diluted with saturated NH₄Cl (200 mL) then extracted several times with EA (20 mL), vigorously shaken for 3 min. The combined organics were washed with brine, dried over anhydrous Na₂SO₄, and then purified by chromatography on silica gel and eluted with PE afford S2 (18.6 g, 93 % yield) as white solid.

Synthesis of compound S3: A Two-necked flasks was charged with compound S2 (10 g, 29.1 mmol), dimethylamine (7.9 g, 0.17 mol), Copper(I) iodide (1.1 g, 5.82 mmol), L-Proline (1.3 g, 11.6 mmol), Potassium carbonate (8.3 g, 59.9 mmol). The flask was evacuated and backfilled with Ar for three times. Dimethyl sulfoxide (80 mL) was added via syringe through the septum. The reaction mixture was heated to 130 °C for 12 h, then it was allowed to cool to room temperature. It was then diluted with saturated NH₄Cl (200 mL) then extracted several times with EA (20 mL), vigorously shaken for 3 min. The combined organics were washed with brine, dried over anhydrous Na₂SO₄, and then the residue was purified by chromatography on silica gel eluted with PE/EA (v/v = 10/1) afford S3 (5.2 g, 52 % yield) as Clear oil.

Synthesis of compound SN-1: Compound S3 (500 mg, 1.8 mmol), benzaldehyde (1000 mg, 9.0 mmol), p-Toluenesulfonic acid monohydrate (342 mg, 1.8 mmol) and acetic acid

(1 mL) was added in a Pressure tube at 140 °C for 12 h. Then, allowed the reaction to cool to room temperature and diluted with saturated NaHCO₃ (50 mL) then extracted several times with DCM (10 mL), vigorously shaken for 3 min. The combined organics were washed with brine, dried over anhydrous Na₂SO₄, and then chloranil (384 mg, 2.0 mmol) was added at room temperature for 30 minutes. The residue was purified by chromatography on silica gel eluted with DCM/MeOH (v/v = 15/1) to afford SN-1 (200 mg, 40 % yield) as black solid. ¹H NMR (400 MHz, CDCl₃) δ 7.83 (d, *J* = 8.0 Hz, 1H), 7.58 (d, *J* = 2.0 Hz, 2H), 7.57 (s, 1H), 7.34 (d, *J* = 9.6 Hz, 2H), 7.29 (s, 2H), 7.03 (d, *J* = 8.0 Hz, 1H), 6.91 (d, *J* = 9.6 Hz, 2H), 3.31 (s, 12H). ¹³C NMR (101 MHz, CDCl₃) δ 159.4, 153.2, 144.5, 137.9, 136.1, 135.4, 129.3, 129.0, 128.6, 127.9, 126.1, 118.9, 115.1, 105.9, 40.7.

Synthesis of compound SN-2: Compound S3 (500 mg, 1.8 mmol), 3-furaldehyde (865 mg, 9.0 mmol), p-Toluenesulfonic acid monohydrate (342 mg, 1.8 mmol) and acetic acid (1 mL) was added in a Pressure tube at 140 °C for 12 h. Then, allowed the reaction to cool to room temperature and diluted with saturated NaHCO₃ (50 mL) then extracted several times with DCM (10 mL), vigorously shaken for 3 min. The combined organics were washed with brine, dried over anhydrous Na₂SO₄, and then chloranil (384 mg, 2.0 mmol) was added at room temperature for 30 minutes. The residue was purified by chromatography on silica gel eluted with DCM/MeOH (v/v = 15/1) to afford SN-2 (150 mg, 30 % yield) as black solid. ¹H NMR (400 MHz, CDCl₃) δ 7.76 (s, 1H), 7.73 (d, *J* = 4.0 Hz, 2H), 7.62 (s, 1H), 7.21 (d, *J* = 2.0 Hz, 2H), 7.00 (dd, *J* = 9.6, 2.4 Hz, 2H), 6.57 (s, 1H), 3.31 (s, 12H). ¹³C NMR (101 MHz, CDCl₃) δ 153.4, 151.5, 144.3, 142.5, 138.5, 135.9, 128.3, 126.2, 119.8, 119.3, 115.4, 113.3, 106.0, 40.9.

Synthesis of compound SN-3: Compound S3 (500 mg, 1.8 mmol), 3-thiophenecarboxaldehyde (1000 mg, 9.0 mmol), p-Toluenesulfonic acid monohydrate (342 mg, 1.8 mmol) and acetic acid (1 mL) was added in a Pressure tube at 140 °C for 12 h. Then, allowed the reaction to cool to room temperature and diluted with saturated NaHCO₃ (50 mL) then extracted several times with DCM (10 mL), vigorously shaken for 3 min. The combined organics were washed with brine, dried over anhydrous Na₂SO₄, and then chloranil (384 mg, 2.0 mmol) was added at room temperature for 30 minutes. The residue was purified by chromatography on silica gel eluted with DCM/MeOH (v/v = 15/1) to afford SN-3 (135 mg, 27 % yield) as black solid. ¹H NMR (400 MHz, CDCl₃) δ 7.63 (d, *J* = 8.0 Hz, 1H), 7.51 (d, *J* = 8.0 Hz, 2H), 7.43 (d, *J* = 4.0 Hz, 1H), 7.37 (d, *J* = 4.0 Hz, 2H), 7.14 (d, *J* = 8.0 Hz, 1H), 6.97 (dd, *J* = 4.0, 4.0 Hz, 2H), 3.35 (s, 12H). ¹³C NMR (101 MHz, CDCl₃) δ 155.5, 153.4, 144.5, 136.1, 135.3, 129.5, 128.3, 127.2, 126.6, 126.2, 119.4, 115.3, 106.1, 40.9.

1.4 Detection of ROS production in solution.

Compound 2',7'-dichlorodihydrofluorescein (DCFH) was used as indicator for detection of ROS in solution. When ROS is generated in the system, the non-fluorescent DCFH will be oxidized and emit obvious fluorescence at 522 nm. 10 μM of SN derivatives and MB were dissolved in 1 mL PBS buffer solution containing 40 μM of

DCFH. The mixture was then placed in a cuvette and irradiated with a LED light at 15 mW/cm². The fluorescence intensity change of the sample at 522 nm was recorded by the fluorescence spectrometer.

1.5 Detection of ¹O₂ production in solution.

Compound 9,10-anthracenediyl-bis(methylene)-dimalonic acid (ABDA) was used as indicator for detection of ¹O₂ in solution. When ¹O₂ is generated in the system, the ABDA will be oxidized and the absorption at 378 nm decrease. 50 μM of SN derivatives and RB were dissolved in 2 mL PBS containing 500 μM of ABDA. The mixture was then placed in a cuvette and irradiated with a LED light at 15 mW/cm². The absorption change of sample at 378 nm was recorded by the UV-Vis absorption spectrophotometer.

1.6 Detection of O₂^{•-} production with DHE in solution.

Droethidium (DHE) was used as indicator for detection of O₂^{•-} in solution. When O₂^{•-} is generated in the system, DHE can be oxidized to form ethidium which intercalates into DNA and emits bright fluorescence at ~580 nm. 10 μM of SN derivatives and NR were dissolved in 1 mL DMSO solvent containing 10 μM of DHE and 70 μg/mL ctDNA. The mixture of SN derivatives were then placed in a cuvette and irradiated with a LED light at 15 mW/cm². The mixture of NR was irradiated with a LED light (450 nm, 62 mW/cm²). The fluorescence decrease of DHE at 420 nm was recorded by the fluorescence spectrometer.

1.7 Cyclic Voltammetry Measurement.

Cyclic voltammograms experiment was conducted by using three-electrode system. A platinum-carbon compound electrode was used as working electrode, the Pt wire electrode and the Ag/Ag⁺ electrode were used as the auxiliary electrode and reference electrode, respectively. The measurement was conducted in dichloromethane containing 0.1 M PBS. The scan range was determined from -1.6 V to 0.6 V and the scan rate was optimized as 20 mV/s. [Fe(CN)₆]³⁻/[Fe(CN)₆]⁴⁻ was used as external reference.

1.8 Photocurrent experiment.

Photocurrent experiments were performed using a conventional three-electrode cell system and an electrochemical workstation (CHI660E, Chenhua, China). The prepared electrode was employed as the working electrode. Meanwhile, a saturated Ag/AgCl electrode and a platinum electrode served as the reference and counterelectrode, respectively. MAX-302 xenon lamp (Asahi Spectra) equipped with an ultraviolet cut-filter (> 420 nm) was used as light source to provide a visible light. i-t curves were measured in 0.1 M PBS solution.

1.9 In vitro cytotoxicity.

4T1 cells and HL-7702 cells were cultured in RPMI-1640 medium containing 10 % FBS and antibiotics (100 units/mL penicillin and 100 μg/mL streptomycin) in a

humidified incubator with 5% CO₂ at 37 °C. 4T1 and HL-7702 cells were seeded in 96-well plates. After 24 h of culture, different concentrations of SN derivatives were added and incubated at 37 °C for 5 min in dark. The sample and control wells were washed twice with PBS buffer and then illuminated by a LED light (560-565 nm, 20 mW/cm²) for 10 min. After incubation at 37 °C for 24 h, the cell viability was examined by cell counting kit-8 (CCK-8) assays. Eliminated of light and the other procedures were the same as dark cytotoxicity.

1.10 Hemolysis assay.

Fresh mouse blood was collected and treated with heparin sodium to prevent blood coagulation. The red blood cells were collected by centrifugation at 5000 rpm for 10 min and then resuspended in PBS (20%, v/v). The 50 µL red blood cell suspension was mixed with 150 µL PBS solution containing different SN-3 concentrations (0.5, 1, 2 and 5 µM). The mixture was incubated at 37°C for 2 h. After centrifugation at 2,000 rpm for 10 min, the OD₅₄₀ of the supernatant was measured by a microplate reader. An untreated red blood cell suspension was used as a negative control, sterile water was used as a positive control, and PBS was used as a solvent control. The hemolysis ratio (%) was calculated as follows: $(OD_{540 \text{ test}} - OD_{540 \text{ negative}}) / (OD_{540 \text{ positive}} - OD_{540 \text{ negative}}) \times 100\%$.

1.11 Confocal co-localization.

4T1 cells were seeded in confocal dishes and incubated for 24 h. 4T1 cells were first incubated with 1 mL RPMI-1640 containing Mito Tracker Green (500 nM, stock solution: 1 mM in DMSO), Endoplasmic reticulum Tracker Green, Lipid droplets Tracker Green and Lysosomes Tracker Green for 20 min, the medium was removed. After washed with PBS for three times and then stained with RPMI-1640 containing 1 µM SN derivatives (stock solution: 5 mM in DMSO) for 5 min, removed the medium and washed with PBS for three times. The cells were imaged using CLSM. For SN derivatives, the excitation was 543 nm and the emission filter was 570-700 nm; For MitoTracker Green, the excitation was 488 nm, and the emission filter was 500-550 nm.

1.12 Intracellular ROS assay.

DCFH-DA was used as an indicator to detect intracellular ROS production under light conditions. 4T1 cells were seeded in confocal dishes for 24 h. Following incubation with 1 mL RPMI-1640 containing SN-3 (1 µM, stock solution: 5 mM in DMSO) for 5 min in the dark. Cells were washed twice with PBS and then DCFH-DA (20 µM) was loaded into the cells for 30 min incubation. Cells were washed twice with PBS and then exposed to light (560-565 nm, 20 mW/cm²) for 10 min. The fluorescence images of treated cells were acquired using CLMS. The DCFH-DA was excited at 488 nm and the emission was collected at 500-530 nm. No background fluorescence of cells was detected under the setting condition.

1.13 Intracellular O₂^{-•} assay.

DHE was oxidized by superoxide anion and bound to DNA to produced red fluorescence. 4T1 cells were seeded in confocal dishes for 24 h. RPMI-1640 containing DHE (10 μM) was first incubated with cells for 30 min in the dark, washed twice with PBS, then incubated with RPMI-1640 containing SN-3(1 μM, stock solution: 5 mM in DMSO) for 5 min and washed, and finally illuminated (560-565 nm, 20 mW/cm²) for 10 min. For DHE, the excitation was 514 nm, and the emission filter was 600 - 650 nm.

1.14 Intracellular ¹O₂ assay.

SOSG as an intracellular ¹O₂ detector. 4T1 cells were seeded in confocal dishes for 24 h. RPMI-1640 containing SOSG (20 μM) was first incubated with cells for 30 min in the dark, washed twice with PBS, then incubated with RPMI-1640 containing SN-3(1 μM, stock solution: 5 mM in DMSO) for 5 min and washed, and finally illuminated (560-565 nm, 20 mW/cm²) for 10 min. For SOSG, the excitation was 488 nm, and the emission filter was 500 - 530 nm.

1.15 Calcein-AM /PI staining of live/dead cell induced by PDT.

4T1 cells were seeded in confocal dishes for 24 h. RPMI-1640 containing SN-3 (1 μM, stock solution: 5 mM in DMSO) was first incubated with cells for 5 min in the dark, washed twice with PBS, then incubated with RPMI-1640 containing AM (1 μM) and PI (1 mg/ml) for 30 min and washed, and finally illuminated (560-565 nm, 20 mW/cm²) for 10 min. For Calcein-AM, the excitation was 488 nm, and the emission filter was 490 - 540 nm; For PI, the excitation was 543 nm, and the emission filter was 610 - 650 nm.

1.16 Mitochondrial depolarization assay.

4T1 cells were seeded and cultured in confocal dishes for 24 h. 4T1 cells were divided into 4 groups: 1) control; 2) light (560-565 nm; 20 mWcm⁻², 10 min); 3) 1 μM SN-3 for 5 min; 4) 1 μM SN-3 for 5 min and light (560-565nm; 20 mW/cm², 10 min); Healthy cell with high mitochondrial membrane potential shows red fluorescent (JC-1 aggregates) and apoptotic cell with a low mitochondrial membrane potential shows green fluorescent (JC-1 monomer). JC-1 monomer: E_x = 488 nm, E_m = 505-545 nm; JC-1 aggregate: E_x = 488 nm, E_m = 560-590 nm.

1.17 poptosis detected by flow cytometry.

Cells were inoculated in 12-well plates and incubated for 24h. The RPMI-1640 was then replaced with fresh medium containing SN-3 (1 μM) and incubated for 5 min. Then, the cells were irradiated with a LED light (560-565 nm, 20 mW/cm²) for 10 min. After further incubation for 12 h, the cells were collected and treated with

AnnexinV-FITC/PI cell apoptosis detection kit. The flow cytometry was used to detect cell apoptosis.

1.18 Subcutaneous tumor model.

All mice were kept in SPF-level feeding conditions with adequate water and food. The temperature is kept at 26 °C, the humidity is 50 % and a 12 hours light / dark cycle. Female mice (BALB/c, 6 - 8 weeks old) were inoculated subcutaneously with homograft tumors. Mice bearing of 4T-1 were injected subcutaneously with 1×10^7 cells into the armpits to establish the breast tumor model. Tumor growth was measured using a caliper, and tumor volume was calculated using the formula: tumor volume = width \times width \times length/2. When tumors reached an average volume of 150 mm³, mice were used for *in vivo* imaging and PDT evaluation.

1.19 In vivo PDT experiments.

All mice were randomly divided into three groups: PBS, SN-3, SN-3+L groups. SN-3 (2.5 mM, 50 μ L/100 mm³ tumor) was injected into the tumors *in situ*. After 2 hours, mice in SN-3+L group were irradiated (532 nm, 100 mW/cm²) for 10 minutes, while SN-3 group were not irradiated. Tumor volumes were measured every 2 days. After 14 days post-PDT, the mice were sacrificed and the tumors and the major organs (liver, spleen, kidney, heart and lung) of the mice were harvested. All collected tissues were fixed in 4 % paraformaldehyde for histological analysis, which were then processed into paraffin, sliced at a thickness of 5 mm for further analysis.

1.20 Histological analysis.

The sections were stained with hematoxylin-eosin (H&E) staining and terminal deoxynucleotidyl transferase dUTP nick end labeling (TUNEL) and finally examined by using an optical microscope (BX51, Olympus, Japan).

1.21 Statistical analysis.

Statistical analysis was performed using GraphPad Prism 8 software. All dates are presented as mean \pm standard deviation (SD) with n = 3, unless specific stated. Differences between groups were determined using Student's t-test or one-way analysis of variance (ANOVA). NS means non-significant, *P < 0.05, **P < 0.01, and ***P < 0.001 were statistically significant.

Supplemental Figures and Tables

Figure S1. ^1H NMR spectrum of SN-1 in CDCl_3 .

Figure S2. ^{13}C NMR spectrum of SN-1 in CDCl_3 .

Figure S3. ^1H NMR spectrum of SN-2 in CDCl_3 .

Figure S4. ^{13}C NMR spectrum of SN-2 in CDCl_3 .

Figure S5. ^1H NMR spectrum of SN-3 in CDCl_3 .

Figure S6. ^{13}C NMR spectrum of SN-3 in CDCl_3 .

Figure S7. High-resolution MALDI-TOF spectrum of SN-1 (MALDI-TOF, m/z: Calcd, 359.1577; Found, 359.1559 (M^+)).

Figure S8. High-resolution MALDI-TOF spectrum of SN-2 (MALDI-TOF, m/z: Calcd, 349.1370; Found, 349.1359 (M^+)).

Figure S9. High-resolution MALDI-TOF spectrum of SN-3 (MALDI-TOF, m/z: Calcd, 365.1141; Found, 365.1133 (M^+)).

Figure S10. Normalized absorption spectrum and PL spectrum of SN PSs in PBS.

Figure S11. Absorption spectra of SN PSs with different concentrations and linear fit of absorbance at the maximum absorption wavelength to its concentration.

Figure S12. PL spectrum changes of the ROS indicator DCFH mixed with SN PSs upon different light irradiation time.

Figure S13. Uv-vis absorption spectra changes of the $^1\text{O}_2$ indicator ABDA mixed with SN PSs and RB upon different light irradiation time.

Figure S14. PL spectra changes of the O_2^- indicator DHE mixed with SN PSs and NR

upon different light irradiation time.

Figure S15. PL spectrum changes of the ROS indicator DCFH mixed with SN PSs upon different light irradiation time in hypoxia.

Figure S16. ESR spectrum of the $^1\text{O}_2$ mixed with SN PSs.

Figure S17. ESR spectrum of the $\cdot\text{OH}$ mixed with SN PSs.

Figure S18. Cytotoxicity of HL-7702 cell.

Figure S19. Co-localized imaging of endoplasmic reticulum, lipid droplets, and lysosomes with SN-3.

Figure S20. Confocal imaging of intracellular $^1\text{O}_2$.

Figure S21. Hemolysis assay after different treatments: sterile water, PBS, SN-3.

Figure S22. Hematoxylin and eosin staining images of the major organs obtained from the mice after different treatments: PBS, SN-3 and SN-3+L.

Table S1. Photophysical data of all compounds in PBS.

Table S2. Calculated electronic transition energies and $\Delta E_{\text{Sn-Tm}}$ of SN-1, SN-2, and SN-3.

Table S3. Calculated spin-orbit coupling (SOC) constants between singlet and triplet states of SN-1, SN-2, and SN-3.

Table S4. The values of $[\langle\text{Sn}|\text{H}_{\text{SO}}|\text{Tm}\rangle/\Delta E_{\text{SnTm}}]^2$ for the ISC between singlet and triplet states of SN-1, SN-2, and SN-3.

Table S5. Recently published photosensitizers and their IC50.

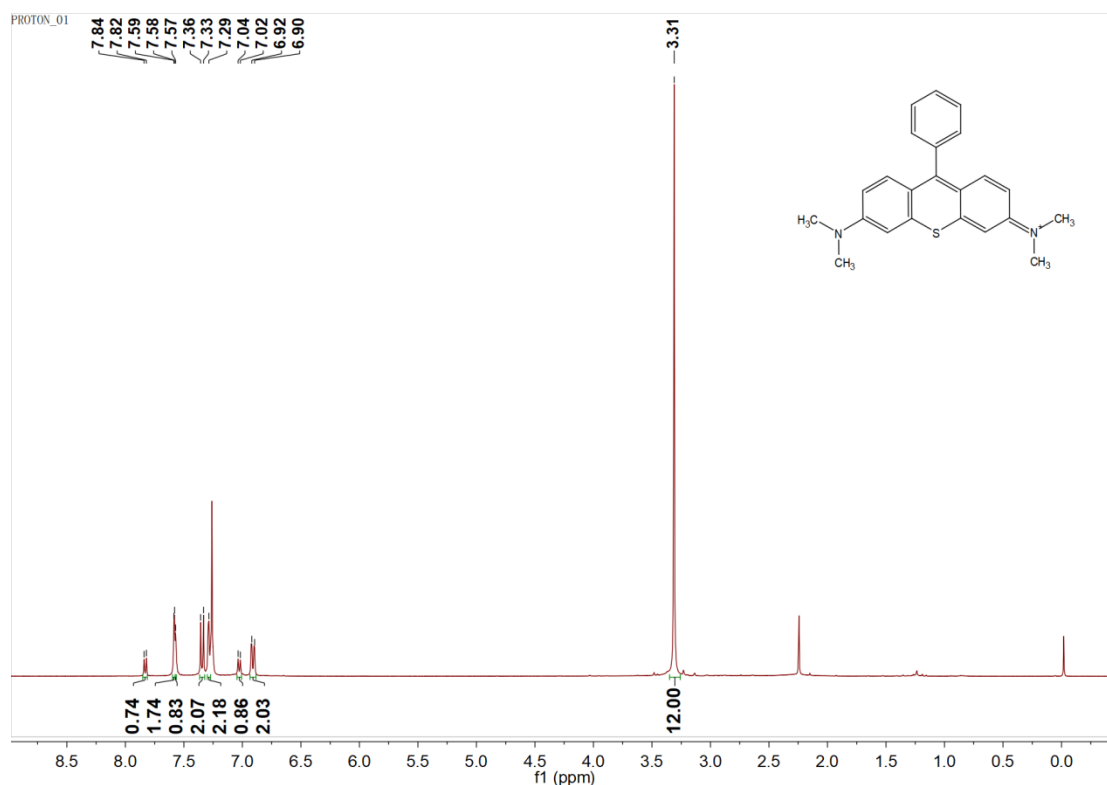


Figure S1. ^1H NMR spectrum of SN-1 in CDCl_3 .

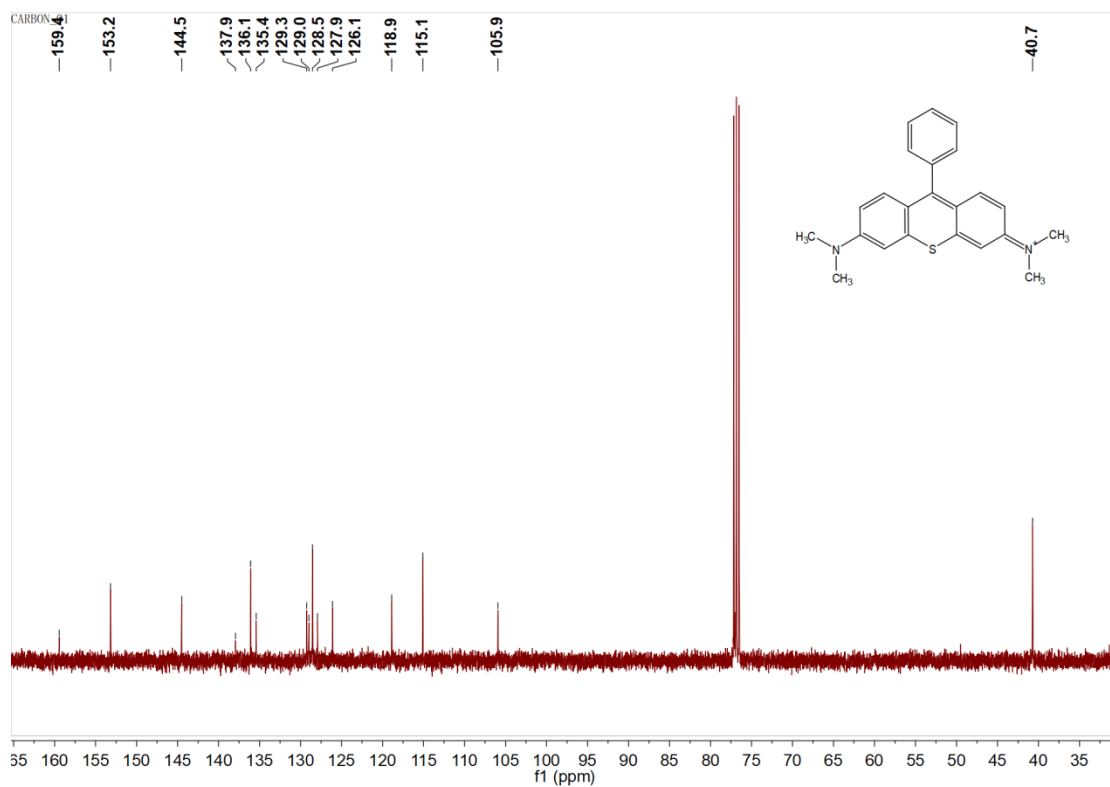


Figure S2. ^{13}C spectrum of SN-1 in CDCl_3 .

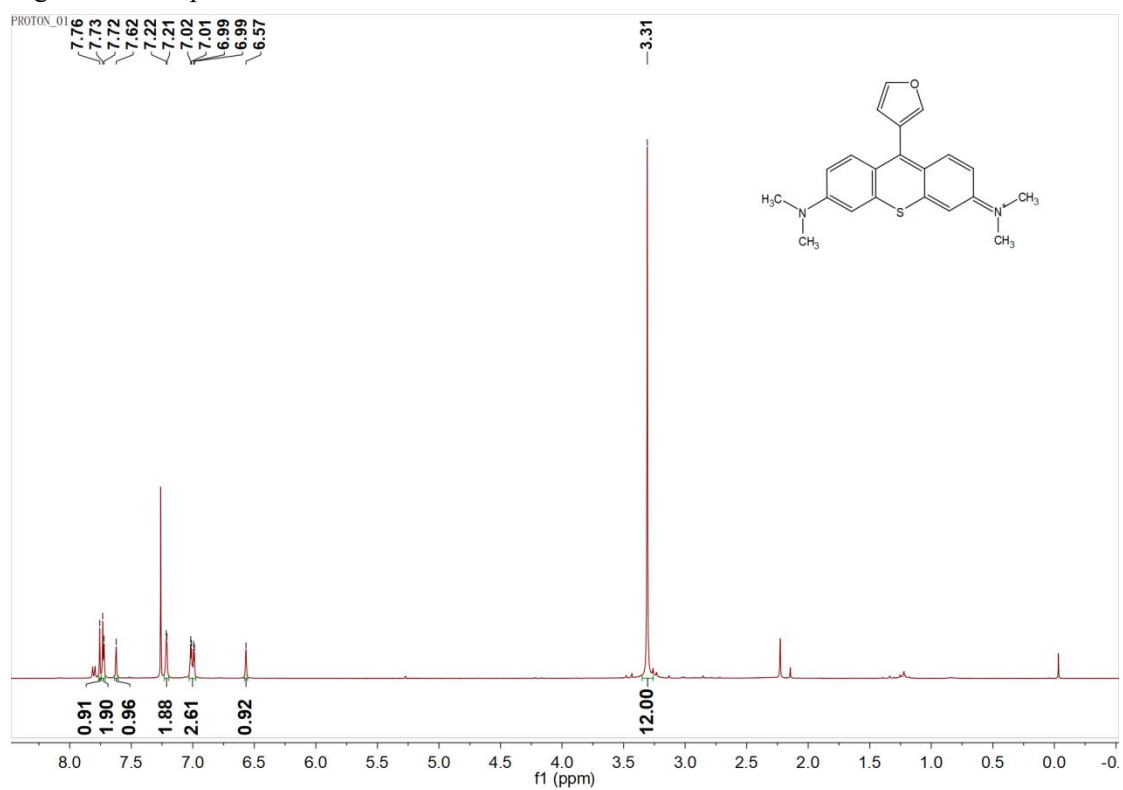


Figure S3. ^1H spectrum of SN-2 in CDCl_3 .

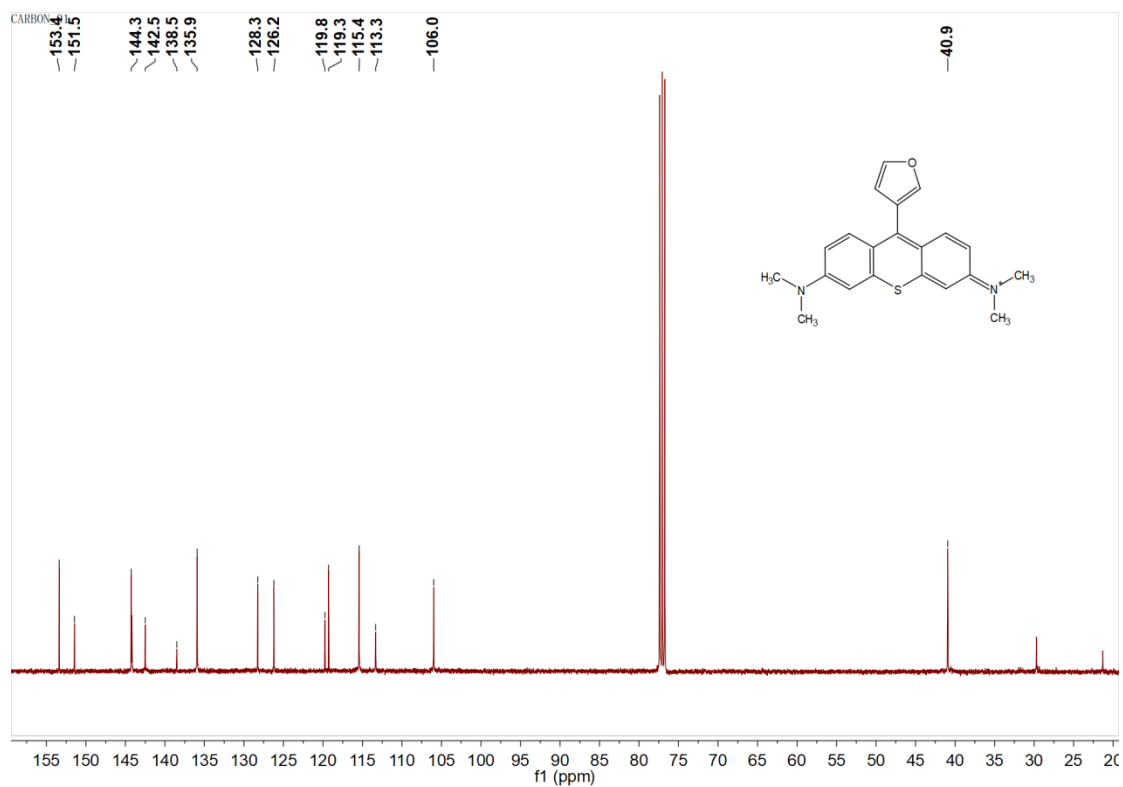


Figure S4. ^{13}C spectrum of SN-2 in CDCl_3 .

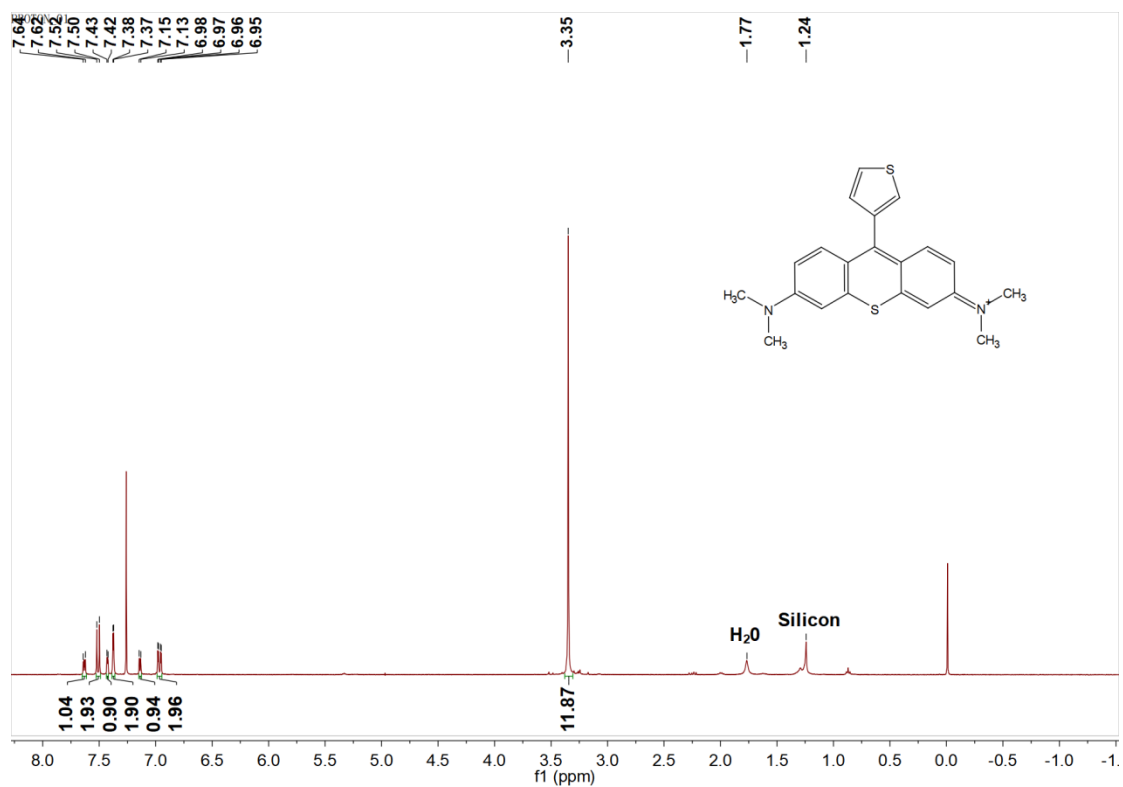


Figure S5. ^1H spectrum of SN-3 in CDCl_3 . The two peaks (1.77, 1.22) should be ascribed to H_2O and impurities in silicone.

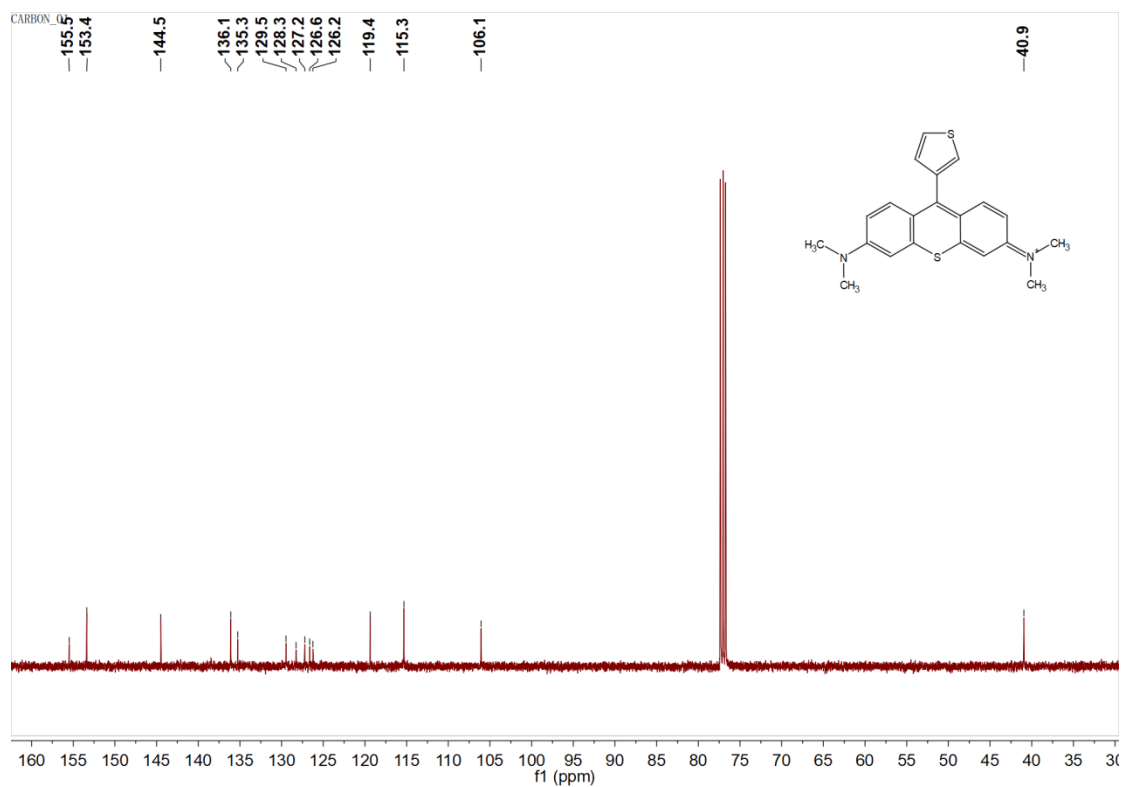


Figure S6. ^{13}C spectrum of SN-3 in CDCl_3 .

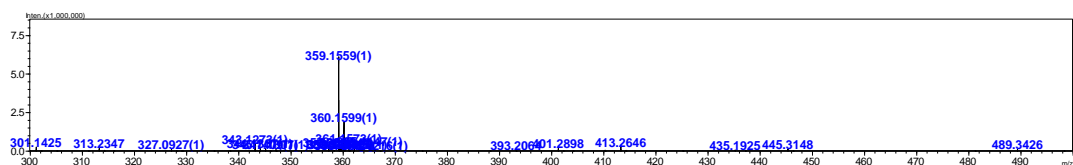


Figure S7. High-resolution MALDI-TOF spectrum of SN-1 (MALDI-TOF, m/z : Calcd, 359.1577; Found, 359.1559 (M^+)).

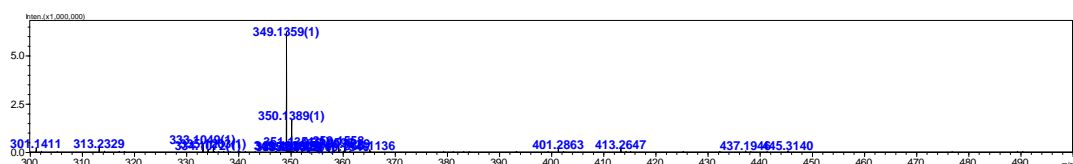


Figure S8. High-resolution MALDI-TOF spectrum of SN-2 (MALDI-TOF, m/z : Calcd, 349.1370; Found, 349.1359 (M^+)).

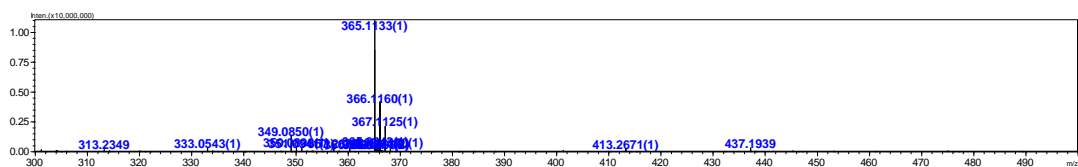


Figure S9. High-resolution MALDI-TOF spectrum of SN-3 (MALDI-TOF, m/z : Calcd, 365.1141; Found, 365.1133 (M^+)).

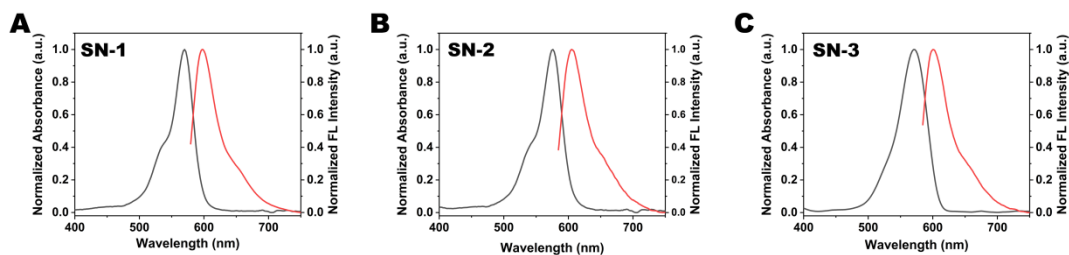


Figure S10. Normalized absorption spectrum and PL spectrum of SN PSs in PBS.

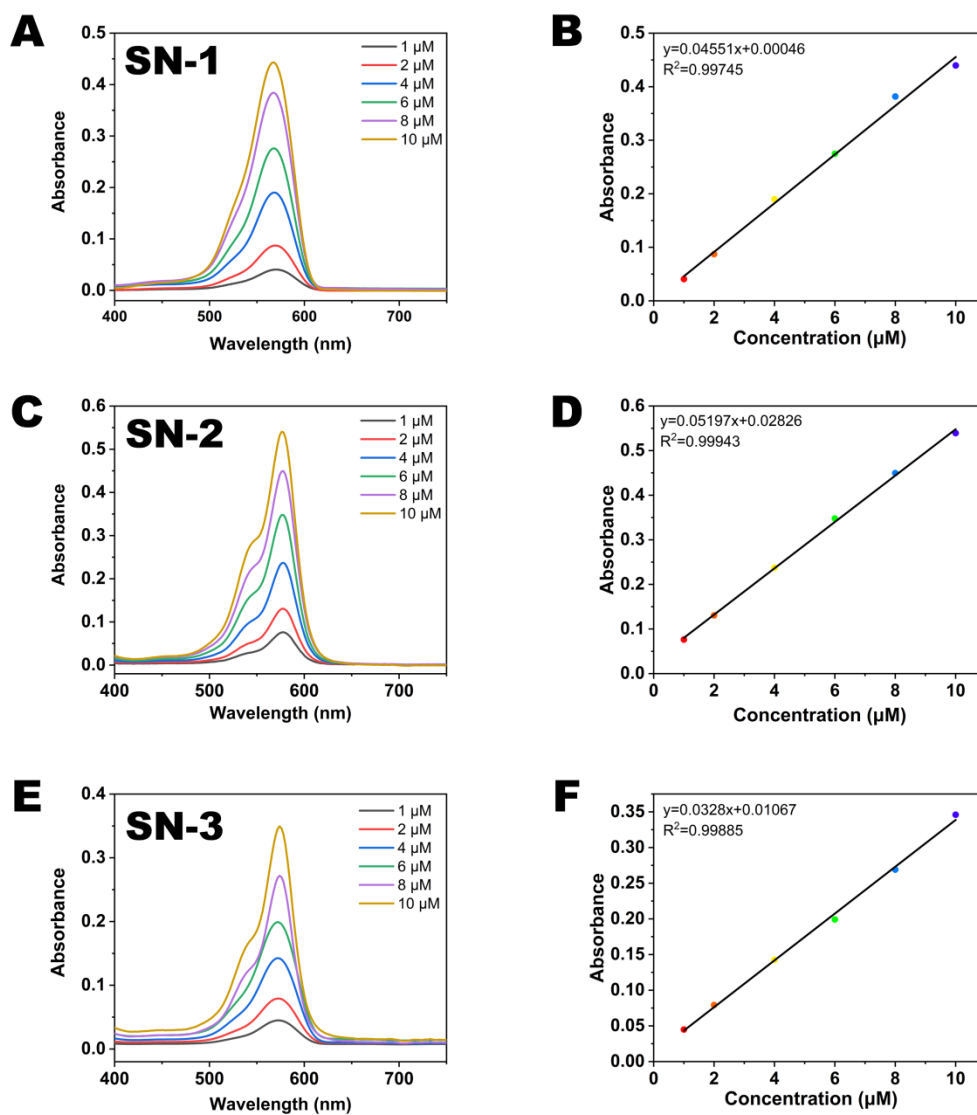


Figure S11. Absorption spectra of SN PSs with different concentrations and linear fit of absorbance at the maximum absorption wavelength to its concentration.

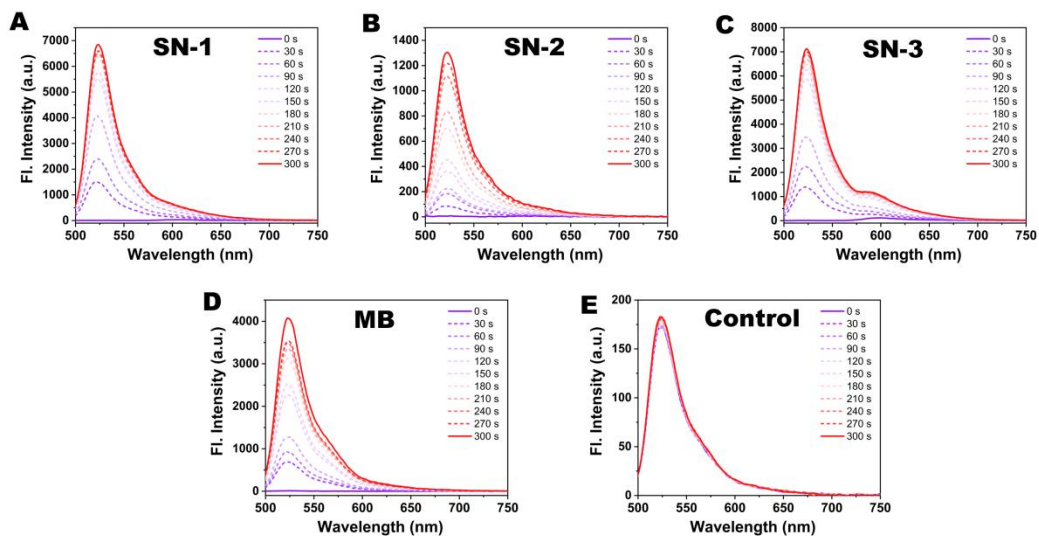


Figure S12. PL spectrum changes of the ROS indicator DCFH mixed with SN PSs and MB upon different light irradiation time.

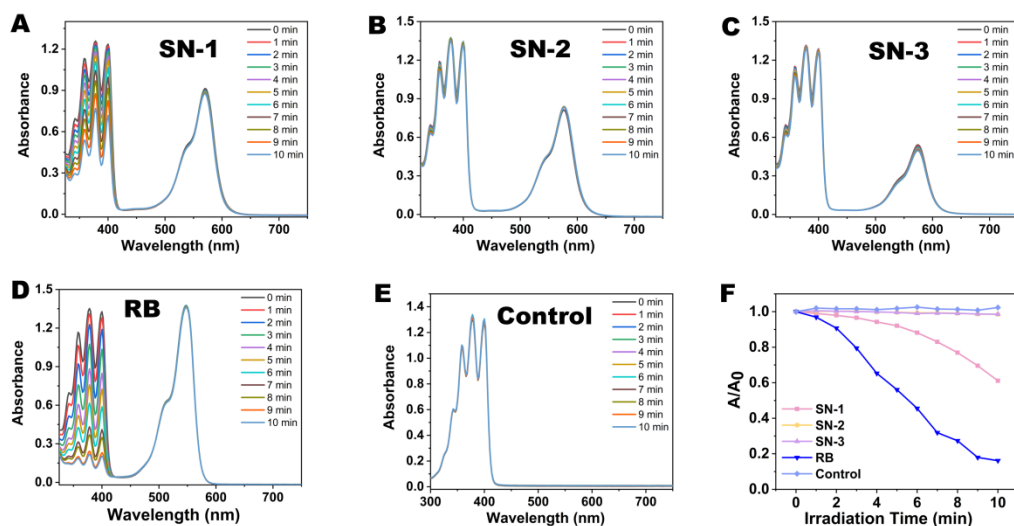


Figure S13. UV-vis absorption spectra changes of the $^1\text{O}_2$ indicator ABDA mixed with SN PSs upon different light irradiation time.

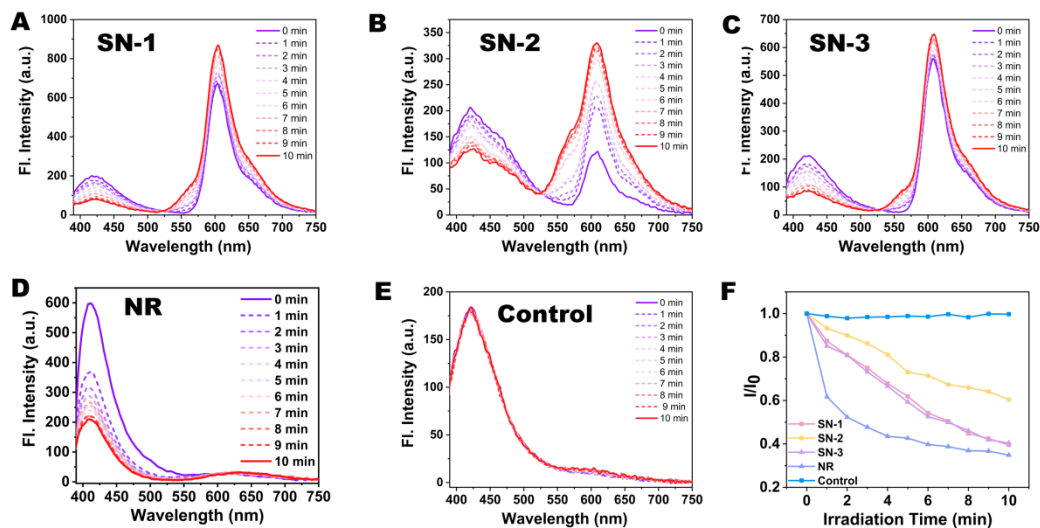


Figure S14. PL spectra changes of DHE in the range of 380-750 nm upon different light irradiation time.

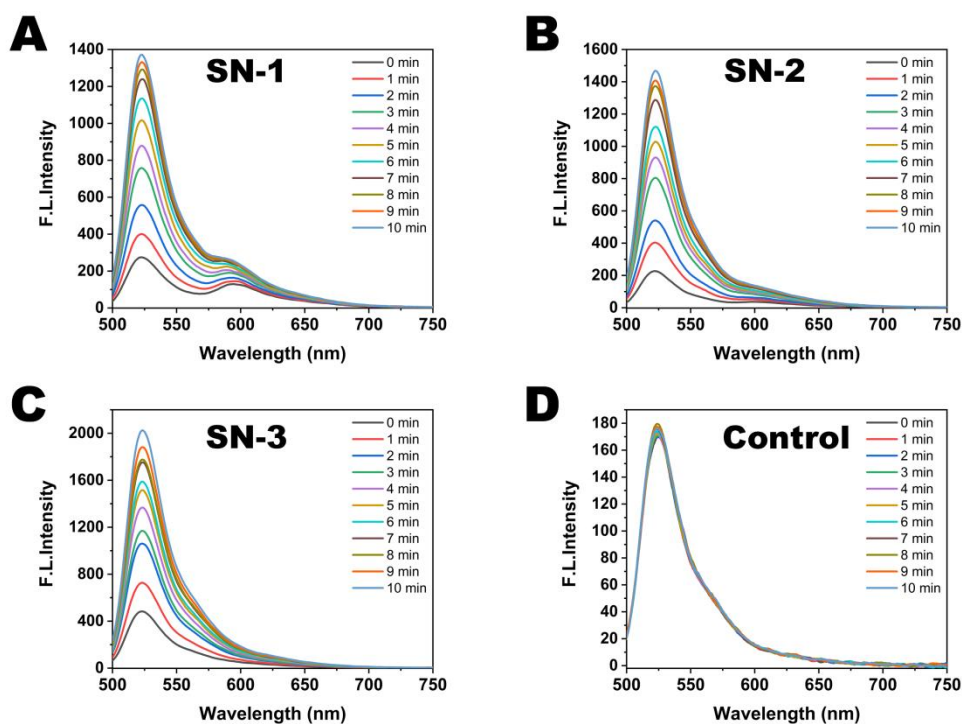


Figure S15. PL spectrum changes of the ROS indicator DCFH mixed with SN PSs upon different light irradiation time in hypoxia.

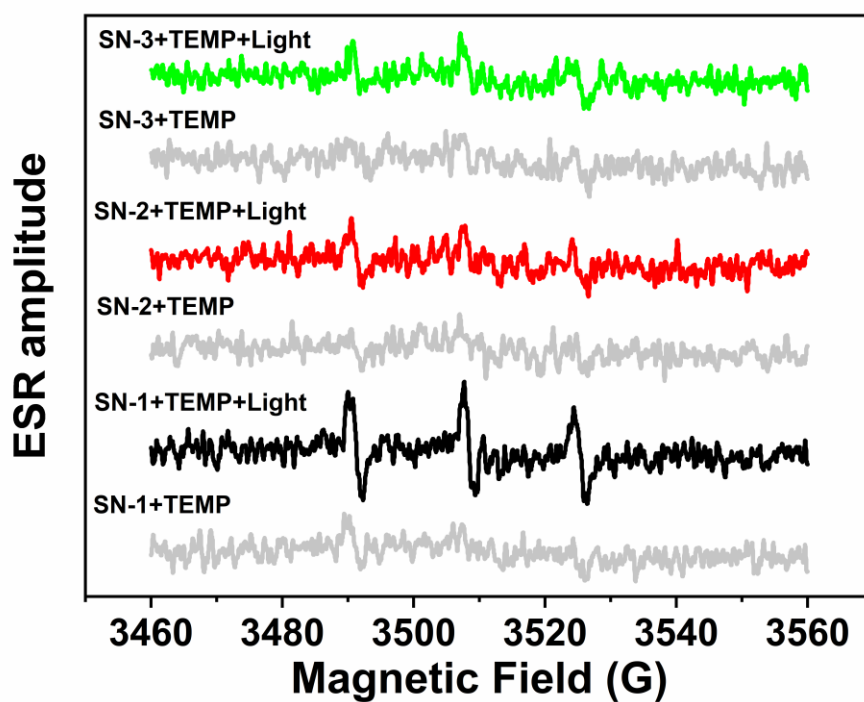


Figure S16. ESR spectrum of the $^1\text{O}_2$ mixed with SN PSs.

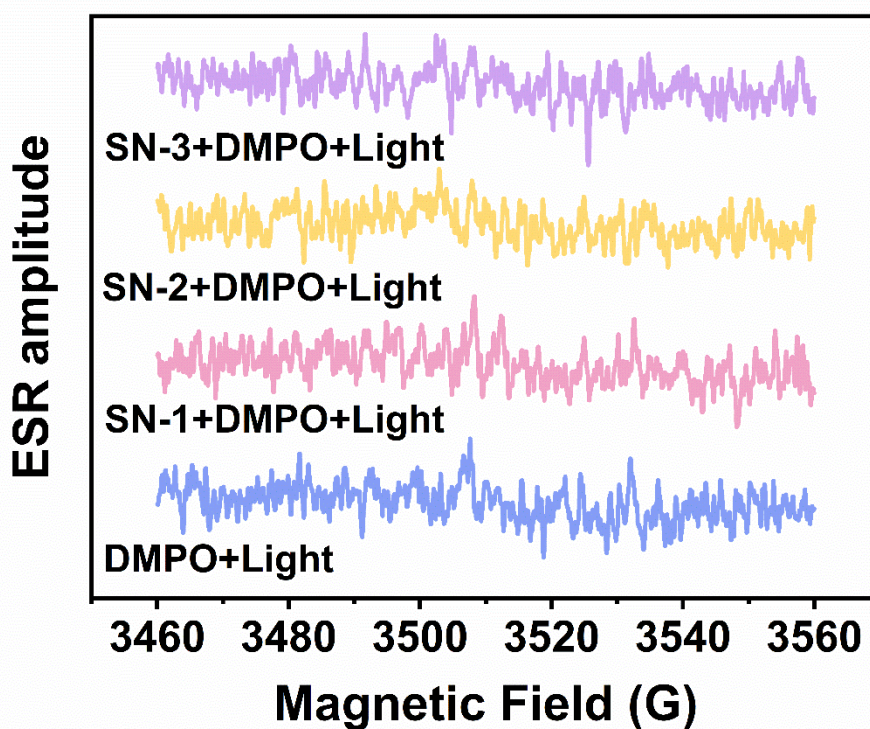


Figure S17. ESR spectrum of the $\cdot\text{OH}$ mixed with SN PSs.

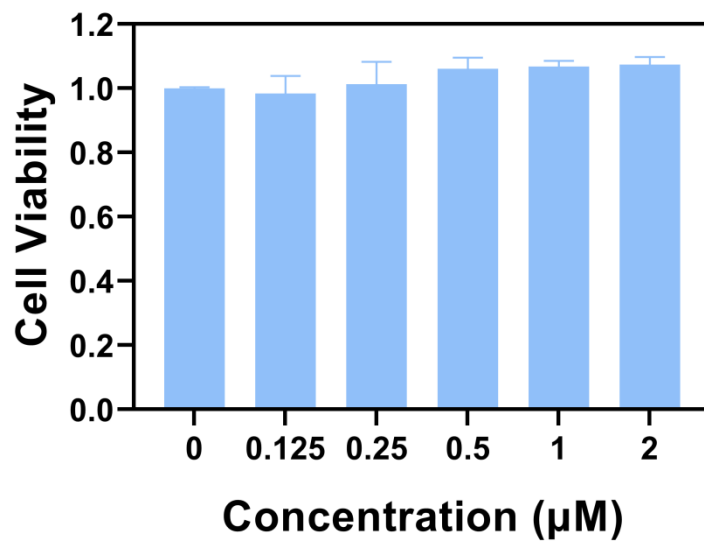


Figure S18. Cytotoxicity of HL-7702 cell.

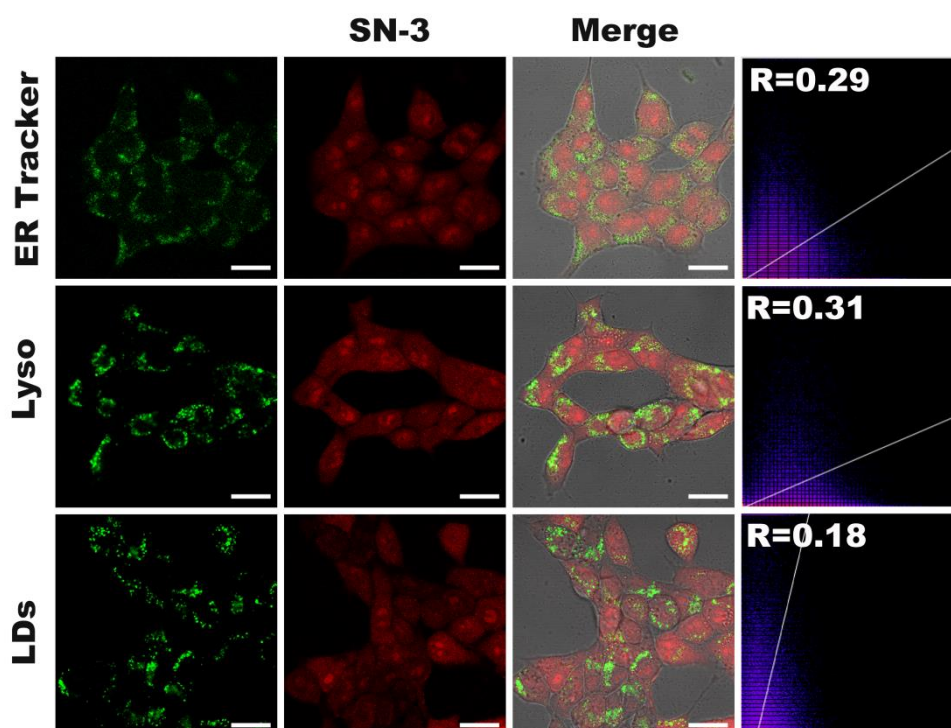


Figure S19. Co-localized imaging of endoplasmic reticulum, lipid droplets, and lysosomes with SN-3. Scale bar: 20 µm

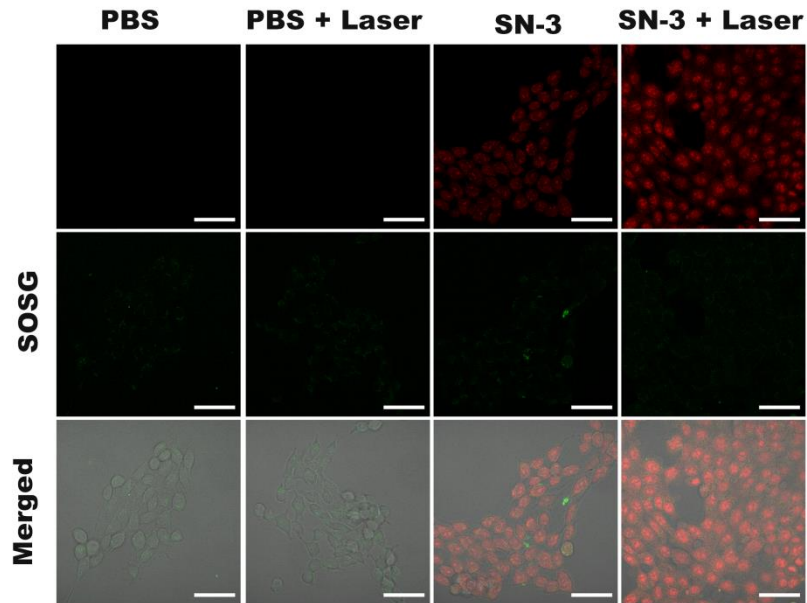


Figure S20. Confocal imaging of intracellular $^1\text{O}_2$. Scale bar: 50 μm

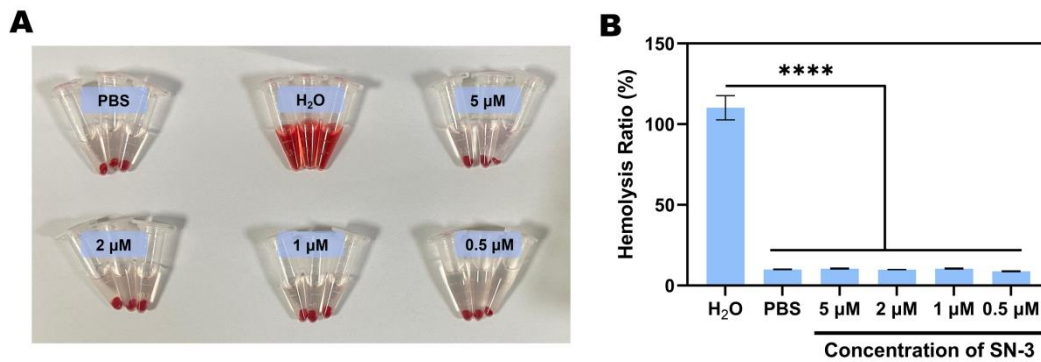


Figure S21. Hemolysis assay after different treatments: sterile water, PBS, SN-3. (n = 3). * $p < 0.05$, ** $p < 0.01$, *** $p < 0.001$, **** $p < 0.0001$, n.s = not significant; one-way analysis of variance.

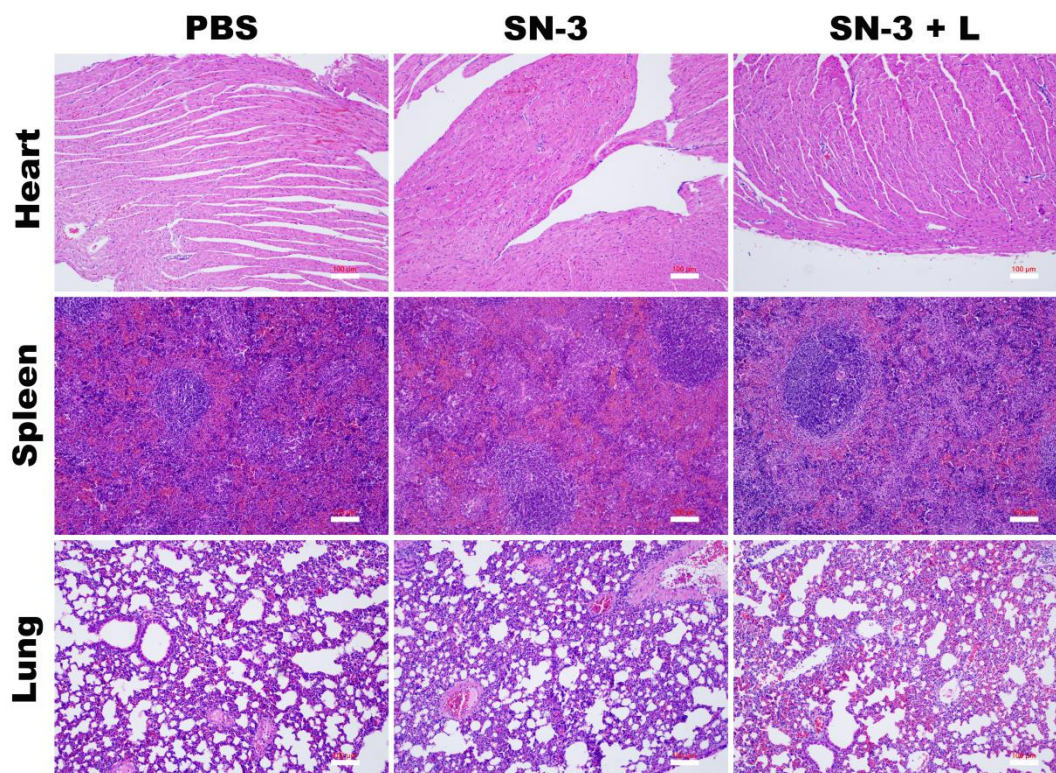


Figure S22. Hematoxylin and eosin staining images of the major organs obtained from the mice after different treatments: PBS, SN-3 and SN-3+L.

Table S1. Photophysical data of all compounds in PBS.

PS	$\lambda_{\text{abs}}(\text{nm})$	$\lambda_{\text{em}}(\text{nm})$	$\epsilon(\text{M}^{-1}\text{cm}^{-1})(\times 10^4)$	$\Phi(\%)$
SN-1	572	600	4.55	16.61
SN-2	576	604	5.20	2.26
SN-3	573	600	3.28	5.00

Table S2. Calculated electronic transition energies and $\Delta E_{\text{S}_n\text{-T}_m}$ of SN-1, SN-2, and SN-3.

Energy (eV)	SN-1	SN-2	SN-3
S ₁	2.568	2.540	2.543
S ₂	2.911	2.873	2.881
S ₃	3.595	3.132	3.286
S ₄	3.847	3.782	3.633
T ₁	1.671	1.656	1.653
T ₂	2.252	2.227	2.231
T ₃	2.864	2.586	2.632
T ₄	3.465	3.052	3.182
$\Delta E_{\text{S}_1\text{T}_1}$	0.897	0.884	0.890

$\Delta E_{S_1T_2}$	0.316	0.313	0.312
$\Delta E_{S_1T_3}$	-0.296	-0.046	-0.089
$\Delta E_{S_1T_4}$	-0.897	-0.512	-0.639
$\Delta E_{S_2T_1}$	1.240	1.217	1.228
$\Delta E_{S_2T_2}$	0.659	0.646	0.650
$\Delta E_{S_2T_3}$	0.047	0.287	0.249
$\Delta E_{S_2T_4}$	-0.554	-0.179	-0.301
$\Delta E_{S_3T_1}$	1.924	1.476	1.633
$\Delta E_{S_3T_2}$	1.343	0.905	1.055
$\Delta E_{S_3T_3}$	0.731	0.546	0.654
$\Delta E_{S_3T_4}$	0.130	0.080	0.104
$\Delta E_{S_4T_1}$	2.176	2.126	1.980
$\Delta E_{S_4T_2}$	1.595	1.555	1.402
$\Delta E_{S_4T_3}$	0.983	1.196	1.001
$\Delta E_{S_4T_4}$	0.382	0.730	0.451

^a $E_{S_nT_m} = \text{Energy}(S_n) - \text{Energy}(T_m)$

Table S3. Calculated spin-orbit coupling (SOC) constants between singlet and triplet states of SN-1, SN-2, and SN-3.

$S_n \langle H_{SO} \rangle T_m$ (cm ⁻¹)	SN-1	SN-2	SN-3
S ₁ -T ₁	0.04	0.09	0.11
S ₁ -T ₂	0.25	0.42	0.32
S ₁ -T ₃	0.11	0.19	0.14
S ₁ -T ₄	0.42	0.32	0.38
S ₂ -T ₁	0.48	0.93	0.74
S ₂ -T ₂	0.12	0.23	0.16
S ₂ -T ₃	0.59	1.43	1.09
S ₂ -T ₄	0.25	1.77	1.96
S ₃ -T ₁	0.29	0.14	0.38
S ₃ -T ₂	2.71	2.30	2.40
S ₃ -T ₃	1.09	0.80	1.53
S ₃ -T ₄	0.44	0.93	4.09
S ₄ -T ₁	0.06	0.19	0.67
S ₄ -T ₂	1.52	1.40	2.00
S ₄ -T ₃	0.43	0.30	3.93
S ₄ -T ₄	0.22	0.75	0.64

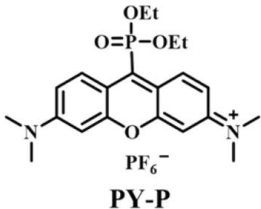
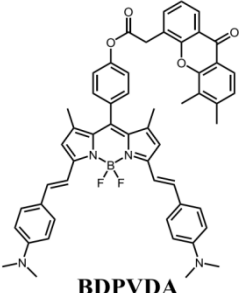
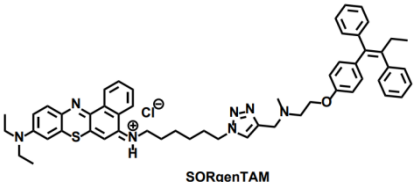
Table S4. The values of $[\langle S_n | H_{SO} | T_m \rangle / \Delta E_{S_nT_m}]^2$ for the ISC between singlet and triplet states of SN-1, SN-2, and SN-3.

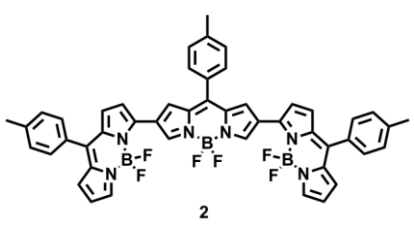
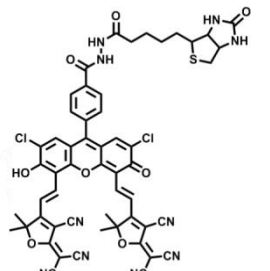
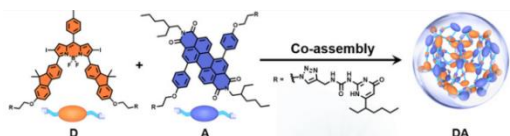
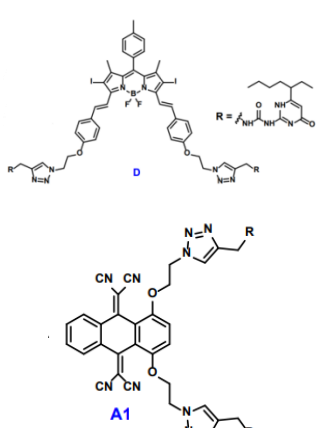
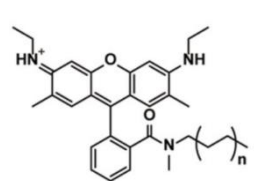
$[\langle S_n H_{SO} T_m \rangle / \Delta E_{S_nT_m}]^2 (\times 10^{10})$	SN-1	SN-2	SN-3
S ₁ -T ₁	0.31	1.59	2.35

S ₁ -T ₂	96.22	276.80	161.71
S ₁ -T ₃	21.23	2622.69	380.39
S ₁ -T ₄	33.07	60.64	55.01
S ₂ -T ₁	23.17	89.95	55.83
S ₂ -T ₂	5.10	19.23	8.77
S ₂ -T ₃	24294.55	3828.42	2933.94
S ₂ -T ₄	31.31	14983.27	6500.14
S ₃ -T ₁	3.41	1.48	8.35
S ₃ -T ₂	626.04	989.58	797.56
S ₃ -T ₃	341.83	333.17	846.03
S ₃ -T ₄	1761.97	20799.00	238260.87
S ₄ -T ₁	0.12	1.23	17.85
S ₄ -T ₂	139.71	125.20	311.47
S ₄ -T ₃	29.78	9.40	2367.76
S ₄ -T ₄	50.25	160.65	307.38
SUM	27458.07	44302.3	253015.41

^aThe values of $R = \frac{[<S_n|H_{SO}|T_m>]}{\Delta E_{S_n T_m}}^2$ are unitless.

Table S5. Recently published photosensitizers and their IC₅₀.

photosensitizer	Type of ROS	IC ₅₀ (μM)	illumination condition	Reference
 <p>PY-P</p>	Type-I	IC ₅₀ Hela = 5.37	590-595nm 50 mW/cm ² 15 min	Chem. Commun., 2022, 58, 7797–7800.
 <p>BDPVDA</p>	Type-I	IC ₅₀ 4T-1 = 2.31 μg/ml	730 nm 100mW/cm ² No mention	Small 2020, 16, 2001059
 <p>SORgenTAM</p>	Type-I	IC ₅₀ MCF-7= 0.0675	660 nm 20 mW/cm ² 5 min	J. Am. Chem. Soc., 2020, 142, 5380–

				5388.
 <p style="text-align: center;">2</p>	Type-I	IC ₅₀ HepG2 = 0.39	730 nm 50 mW/cm ² 10 min	Angew. Chem., Int. Ed., 2021, 60, 19912–19920.
	Type-I	IC ₅₀ MCF-7 = 10.3	white-light 20 mW/cm ² 10 min	Nat. Commun., 2022, 13, 2225.
	Type-I	IC ₅₀ Hela = 0.67 μg/ml	white-LED 40 mW/cm ² 10 min	J. Am. Chem. Soc., 2023, 145, 4081–4087.
	Type-I	IC ₅₀ Hela = 0.88	660 nm 20 mW/cm ² 10 min	Nat. Commun., 2022, 13, 6179.
 <p>n = 0 : Rh19-MA-C2 n = 8 : Rh19-MA-C18</p>	Type-I	IC ₅₀ PC9-luc = 0.17/0.048	520-530 nm 64 J/cm ² 10 min	ACS Appl. Nano Mater., 2022, 5, 14954–14960.